Oil–source correlation for the paleo-reservoir in the Majiang area and remnant reservoir in the Kaili area, South China

Yunxin Fang [a,b], Yuhong Liao [a], Liangliang Wu [a,b], Ansong Geng [a,*]

[a] The State Key Laboratory of Organic Geochemistry, Guangzhou Institute of Geochemistry, Chinese Academy of Sciences, Wushan, Guangzhou 510640, PR China
[b] The Graduate School of Chinese Academy of Sciences, Beijing 100039, PR China

ABSTRACT

There are different viewpoints on the oil-source correlation of the Majiang paleo-reservoir and the neighbouring Kaili remnant reservoir in the Southern Guizhou Depression of China. Three potential source rocks in this depression could be inferred: the Lower-Cambrian marine mudstone, Lower-Silurian shale and Lower-Permian mudstone. Most of the potential source rocks are of high maturity. The solid bitumens and oil seepages in the Southern Guizhou Depression suffered severe secondary alterations, such as thermal degradation and biodegradation. The solid bitumens of the Majiang paleo-reservoir are also of high maturity. The oil seepages and soft bitumen of the Kaili remnant reservoir were severely biodegraded. All these secondary alterations may obscure oil-source correlations by routine biomarkers. Thus, it is very important to select appropriate biomarker parameters for the oil-source correlation. In this work, biomarkers resistant to thermal degradation and biodegradation and the data of organic carbon isotopic compositions were used for the correlation. The $\delta^{13}C$ values of n-alkanes in asphaltene pyrolysates were also used to make oil–oil and oil–source correlations between severely biodegraded oils. The results indicate that the Lower-Cambrian marine mudstones are the main source for the Ordovician–Silurian (O–S) solid bitumens of the Majiang area and the Ordovician–Silurian oil seepages and soft bitumens of the Kaili area. Remnant reservoir in the eastern Kaili area might have been charged at least twice by the oil generated from the Lower-Cambrian marine source rocks.

© 2011 Elsevier Ltd. All rights reserved.

1. Introduction

The Majiang paleo-reservoir is one of the biggest paleo-reservoirs in South China (Fig. 1). It was formed in Caledonian period, typically contains solid pyro-bitumen that was altered by thermal maturation. It was an oil reservoir controlled by both lithologic and structural factors (Wu, 1989). It was about 2450 km² in Caledonian period, but it just covers an area of 800 km² at present, mainly in the Majiang, Duyun and Danzhai area. Only solid bitumens were left in Majiang paleo-reservoir because the reservoir had been destroyed in the continuous tectonic orogenies since Caledonian period. The solid bitumens of the Majiang paleo-reservoir are stored mainly in the pores and structural fissures of the carbonates of Lower-Ordovician Honghuayuan formation (O_1h), the intergranular pores of the sandstones of Lower–Middle Silurian Wengxiang group ($S_{1-2}wx^1$) and the pores of the carbonates of Lower-Permian Maokou formation (P_1m).

The Kaili remnant reservoir is located in the eastern part of the Southern Guizhou Depression. It lies to the east of the Majiang paleo-reservoir (Fig. 1). The Kaili remnant reservoir and the Majiang paleo-reservoir were separated by Guiding-Kaili fault zone. The Kaili remnant reservoir includes three wide multiple synclines of Ordovician–Silurian (Fig. 2). During Yanshanian orogeny to Himalayan orogeny, most of the reservoirs in the Kaili area were outcropped and destroyed. Nevertheless, liquid oils and soft bitumens occur extensively in the O–S reservoirs, such as the oil seepages in Kaitang village and the soft bitumen in Panghai village (Fig. 1).

Previous studies (Ma et al., 2004; Tenger et al., 2008; Chen et al., 2006; Ding et al., 2007; Tian et al., 2006) have provided much information on the geological structure and oil–source correlation in the study area. However, there are still debates on the source rocks of the Ordovician–Silurian (O–S) oil seepages and bitumens in the study area. Some previous workers (Wu, 1989; Tian et al., 2006; Hu et al., 2007; Tenger et al., 2008; Zhang et al., 2007) held the point that the Lower-Ordovician solid bitumens in the Majiang paleo-reservoir and the O–S oil seepages and soft bitumens in the Kaili remnant reservoir were all mainly sourced from the Lower-Cambrian marine mudstones. While Ma et al. (2004) resolved that the Permian source rock of the eastern Kaili area was also one of the source rocks of the O–S oil seepages and soft bitumens in the Kaili remnant reservoir. However, Li et al. (2006) opined that the O–S oil seepages of the Kaili area were sourced both from the Lower-Cambrian marine mudstones and from the source rocks of

* Corresponding author. Tel.: +86 20 87682870, fax: +86 20 85290281.
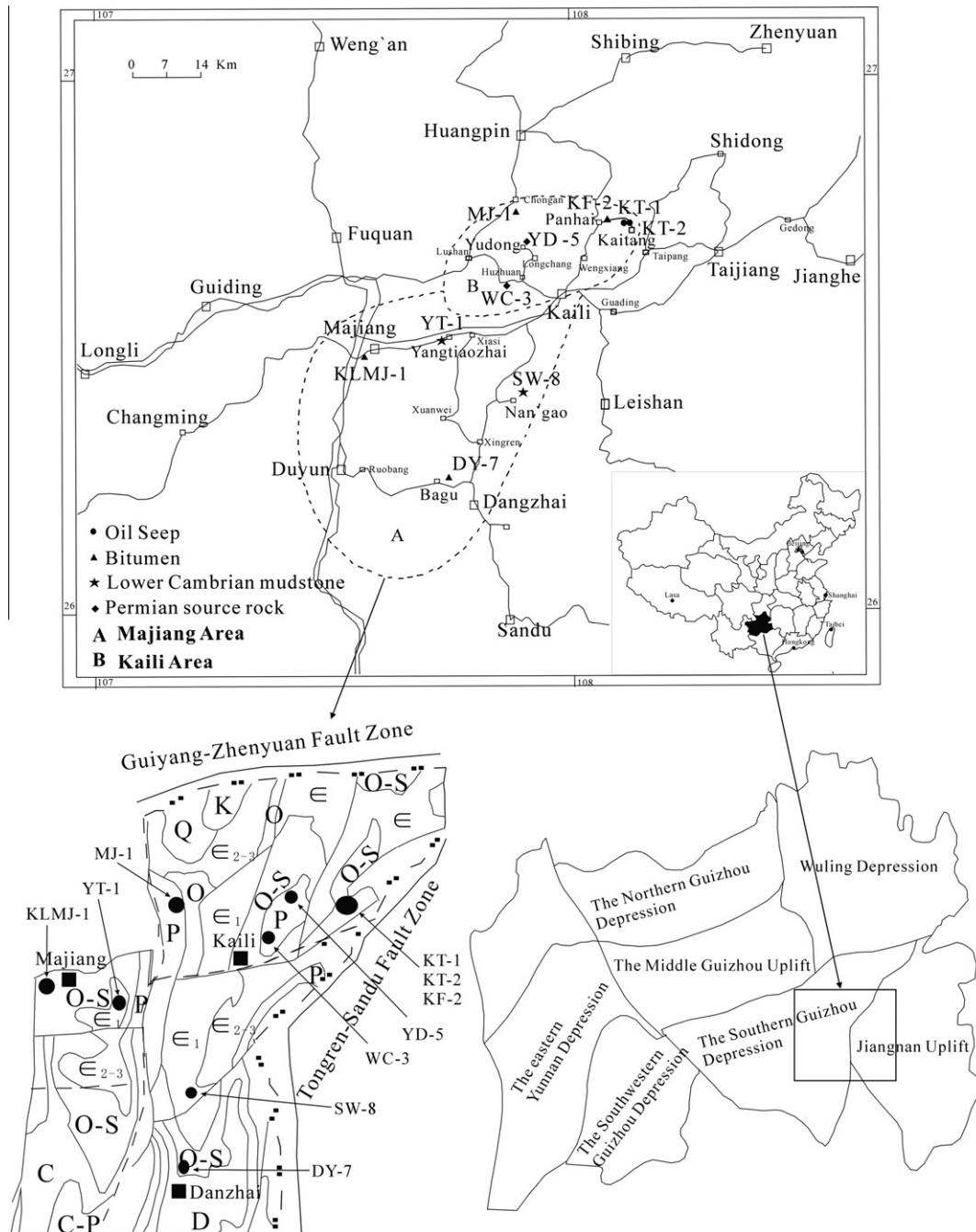E-mail address: asgeng@gzb.ac.cn (A. Geng).

Fig. 1. Map showing sampling locations and the study area. A: the Majing paleo-reservoir, B: the Kaili remnant reservoir.

Lower-Silurian and Lower-Permian. Nevertheless, most of the Lower-Ordovician solid bitumens of the Majiang paleo-reservoir and most of the potential source rocks, except the Permian source rocks in the Kaili area, are over matured. The Ordovician–Silurian oil seepages and Lower-Ordovician soft bitumens of the Kaili remnant reservoir have suffered severe biodegradation. These secondary alterations may influence oil–source and oil–oil correlations by routine biomarkers such as C_{27}–C_{29}-regular steranes and terpanes. Previous studies (Ma et al., 2004; Chen et al., 2006; Ding et al., 2007; Tian et al., 2006; Zhang et al., 2007) in the area failed to eliminate the influence of such secondary alterations. Due to the factors mentioned above, oil–source and oil–oil correlations should be very carefully within the study area.

The purpose of this study is to make oil–source correlation for the paleo-reservoir in the Majiang area and remnant reservoir in

the Kaili area. Biomarkers resistant to thermal degradation and biodegradation coupled with data of organic carbon isotopic compositions were used for the correlation studies. The $\delta^{13}C$ values of n-alkanes in asphaltene pyrolysates were also employed to correlate the severely biodegraded oil seepages.

2. General geological settings and samples

The Southern Guizhou Depression, with an area of 30,000 km^2, is located at Middle and Upper Yangtze region of South China (Fig. 1). Fig. 3 shows the generalized stratigraphic column, petroleum occurrence and potential source rocks of the depression. There exist three potential source rocks with high TOC values (>1%) in this depression, the Lower-Cambrian marine mudstones
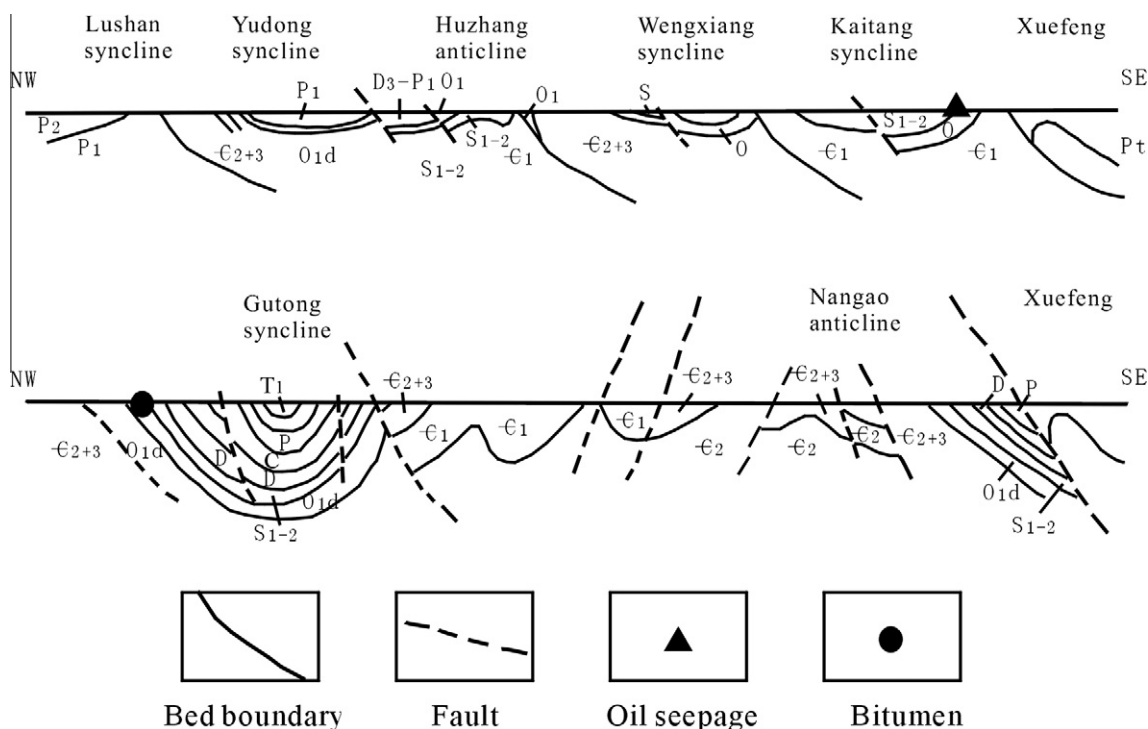
Fig. 2. The geologic cross section of the Majing paleo-reservoir (below) and the Kaili remnant reservoir (above). (Modified from Ma et al., 2004).

of the Niutitang formation ($\in_1 n$) developed in both basin and slope sedimentary environments, the Lower-Silurian shale of the Long-maxi formation ($S_1 l$) and the Lower-Permian mudstones of the Qix-ia formation ($P_1 q$) developed in both basin and lagoonal sedimentary environments (Zhang et al., 2007; Tenger et al., 2008; Li et al., 2006; Liu et al., 2008). The Lower-Cambrian Niuti-tang formation ($\in_1 n$) consists of about 200–300 m of dark marine mudstones in the study area, while the Qixia formation ($P_1 q$) consists of dark mudstones, with a total thickness of 70–175 m (Zhai et al., 1987).

Various samples in the study area have been collected and analyzed, including the potential source rocks from the Lower-Cambrian, Lower-Silurian and Lower-Permian strata, the Lower-Ordovician solid bitumens of the Majiang paleo-reservoir and the Kaili remnant reservoir, the Lower-Ordovician soft bitu-men and Ordovician–Silurian oil seepages of the Kaili remnant reservoir (Figs. 1 and 2; Table 1). The Lower-Silurian shale of Longmaxi formation ($S_1 l$) was presumed as the potential source rock of the O–S oil seepages in the Kaili area (Li et al., 2006). However, the occurrence of the Lower-Silurian shale of the Long-maxi formation was only constrained to the northwestern part of Guizhou Province and it is not represented in the stratigraphic column (Fig. 3). There was neither outcrop nor core sample of the Lower-Silurian Longmaxi formation shale in the eastern Kaili area, even in all the study area. Therefore, the Lower-Silurian shale (SW-1) was sampled as an alternative equivalent from the Xishui area of Guizhou Province, 400 km away from the Majiang area and out of the extent of Fig. 1.

The total organic carbon (TOC) contents of the Lower-Cambrian marine mudstones (YT-1 and SW-8) are over 6%, and TOC of the Lower-Silurian shale (SW-1) is 1.49%. The Ro% values of the Low-er-Cambrian marine mudstones and Lower-Silurian shale are above 2.5% , Ro% values of the Lower-Permian mudstone (WC-3, 2.0%TOC) and the Lower-Permian coal (YD-5, 16%TOC) is 0.67% and 0.58% respectively. Rock–Eval data of the source rocks, and bulk $\delta^{13}C$ values of kerogens, oil seepages and bitumens are pre-sented in Table 1.

The oil seepages of the Kaitang village which belongs to the Kaili remnant reservoir (KT-1 and KT-2) occur in the neighouring disconformable strata. KT-1 was from the Lower-Ordovician mar-lite of the Dawan formation ($O_1 d$) and KT-2 was from the Lower-Middle Silurian coral reef of the Wengxiang group ($S_{1-2}wx^1$) in the Kaitang syncline. The asphaltene contents of KT-1 and KT-2 are 15.6% and 41.4%, respectively. Severe biodegradation should be responsible for the high asphaltene contents. Based on the Rb values of the solid bitumens, the equivalent Ro values of the solid bitumens could be calculated (Jacob, 1985). The equivalent Ro of the soft bitumen KF-2 in Panghai village of the Kaili area is 1.0%. The equivalent Ro values are all over 1.4% for the other three bitu-mens (KLMJ-1 in $O_1 h$, DY-7 in $O_1 h$ and MJ-1 in $P_1 m$). The contents of DCM extractable organic matter (EOM) in the three solid bitu-mens and the source rocks of the Lower-Cambrian and Lower-Silu-rian were all very limited (Table 2).

3. Experimental

3.1. Sample pretreatment and asphaltene pyrolysis

The solid bitumens and source rocks samples were all crushed to 80 mesh and extracted with a mixture of dichloromethane (DCM) and methanol (93:7, v/v) at 46 °C for 72 h. The precipitation and purification of the asphaltenes is similar to that described by Liao et al. (2009). The asphaltenes of the O–S oil seepages KT-1 and KT-2 were sealed in glass tubes under nitrogen and heated at 320 °C for 72 h. After cooling, the glass tubes were opened, and the solid residues were crushed and extracted with DCM. The extracts from source rocks and pyrolysis residues were first depleted of asphaltenes and then fractionated into saturates, aro-matics and resins by successive elution with hexane, hexane/DCM (5:3, v/v) and DCM/MeOH (2:1, v/v) on alumina/silica gel (1:3, v/v) columns respectively. The saturate and aromatic hydro-carbon fractions were analyzed by GC and GC–MS. The $\delta^{13}C$ values of n-alkanes in both the saturate extracts and asphaltene
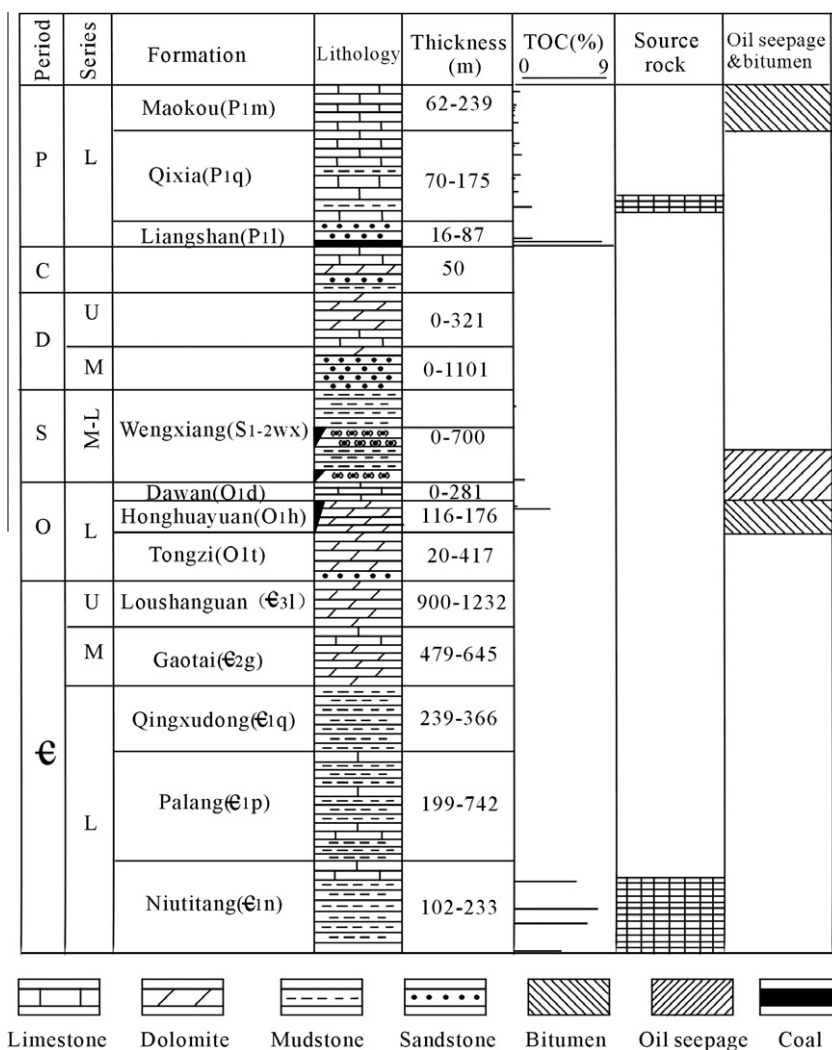
Fig. 3. Stratigraphy, petroleum occurrence and potential source rocks of the Southern Guizhou Depression of China (modified from Tenger et al., 2008).

Table 1
The basic geochemical parameters of the samples in Southern Guizhou Depression.

Sample	Formation	Description	Ro (%)	TOC (%)	T_{max} (°C)	HI	Bulk $\delta^{13}C$ (‰)
SW-8	$\in_1 n$	Mudstone	2.58	6.44	609	2	−32.5
YT-1	$\in_1 n$	Mudstone	–	6.81	608	2	−34.7
SW-1	$S_1 l$	Shale	2.61	1.49	608	1	−29.3
WC-3	$P_1 q$	Mudstone	0.67	2.01	449	130	−28.7
YD-5	P_1	Coal	0.58	16	438	173	−26.2
KT-1	$O_1 d$	Oil seepage	–	–	–	–	−32.2
KT-2	$S_{1-2} wx^1$	Oil seepage	–	–	–	–	−32.3
KF-2	$O_1 h$	Soft bitumen	1	–	442	246	−32.2
KLMJ-1	$O_1 h$	Solid bitumen	–	–	467	70	−32.3
DY-7	$O_1 h$	Solid bitumen	2.1	–	528	51	−32.3
MJ-1	$P_1 m$	Solid bitumen	2.01	–	–	–	−27.9

pyrolysates were measured by GC-C-IRMS. Saturated hydrocarbon fraction was depleted of branched/cyclic hydrocarbons by urea adduction (Liao et al., 2004) prior to the GC-C-IRMS analysis.

3.2. Instrumental

3.2.1. GC–MS

Analysis of the saturate biomarkers was conducted using a Finnigan Trace GC Ultra gas chromatography, equipped with a DB-5 fused silica capillary column (60 m × 0.32 mm i.d. ×0.25 μm film thickness) coupled to a Thermo Fisher DSQ II mass spectrometer. And the GC oven was held isothermally at 70 °C for 2 min, programmed from 70 °C to 140 °C at 6 °C min^{-1} and from 140 °C to 295 °C at 3 °C min^{-1}, with a final holding time of 30 min. The Aromatic hydrocarbon was analyzed by GC–MS with a 60 m × 0.32 mm × 0.25 μm i.d. fused silica HP-5 column, and the temperature program was kept isothermally at 70 °C for 2 min, programmed at a rate of 3 °C min^{-1}–160 °C, and then at a rate of 4 °C min^{-1}–290 °C and finally kept isothermally at 290 °C for 30 min. The ion-source temperature was 250 °C, and the

Table 2
The EOM and bulk fractions parameters of the samples in Southern Guizhou Depression.

Sample	Formation	Description	EOM‰	Saturated%	Aromatic%	Resin%	Asphaltene%	Sat/Aro
SW-8	$\in_1 n$	Mudstone	0.02	30.3	9.1	30.3	30.3	3.33
YT-1	$\in_1 n$	Mudstone	0.04	–	–	–	–	1.40
SW-1	$S_1 l$	Shale	0.08	26.5	32.7	26.5	14.3	0.81
WC-3	$P_1 q$	Mudstone	1.64	25.3	32.1	20.3	22.3	0.79
YD-5	P_1	Coal	6.62	16.1	50.0	7.1	26.8	0.32
KT-1	$O_1 d$	Oil seepage	–	43.3	31.1	10.0	15.6	1.39
KT-2	$S_{1-2}wx^1$	Oil seepage	–	23.4	20.7	14.5	41.4	1.13
KF-2	$O_1 h$	Soft bitumen	44.55	35.3	24.5	8.8	31.5	1.44
KLMJ-1	$O_1 h$	Solid bitumen	0.20	–	–	–	–	4.50
DY-7	$O_1 h$	Solid bitumen	0.66	24.6	14.5	24.6	36.3	1.70
MJ-1	$P_1 m$	Solid bitumen	0.31	10.6	62.4	18.0	9.0	0.17

Table 3
Biomarker assignments.

Peak	Compound
TT20	C_{20}-tricyclic terpane
TT21	C_{21}-tricyclic terpane
TT23	C_{23}-tricyclic terpane
Ts	18α (H)-C_{27}-trisnorhopane
Tm	17α (H)-C_{27}-trisnorhopane
N28	C_{28}-28,30-bisnorhopane
N29	C_{29}-$\alpha\beta$ hopane
H30	C_{30}-$\alpha\beta$ hopane
C21	Pregnane
C22	Homopregnane
C27	C_{27}-$\alpha\alpha\alpha$R sterane
C28	C_{28}-$\alpha\alpha\alpha$R sterane
C29	C_{29}-$\alpha\alpha\alpha$R sterane
C29D	C_{29}-$\beta\alpha$R diasterane

instrument was operated in the electron impact (EI) mode with an electron energy of −70 eV.

3.2.2. GC-C-IRMS

GC-C-IRMS analyses were performed in a VG Isochrom II system. The GC was fitted with a 30 m × 0.32 mm × 0.25 μm i.d DB-1 fused silica capillary column. Helium was used as the carrier gas. The GC was held isothermally at 70 °C for 2 min, programmed from 70 to 160 °C at 6 °C min^{-1} and from 160 to 295 °C at 3 °C min^{-1}, with a final holding time of 25 min. The combustion furnace was held at 850 °C. Carbon isotope ratios of *n*-alkanes were calculated using CO_2 as a reference gas which was automatically introduced into the IRMS at the beginning and end of each analysis, and the data were reported relative to the PDB standard. The standard deviation of GC-C-IRMS for each compound is less than 0.3‰.

4. Results and discussion

4.1. Geochemical characteristics of the potential source rocks

The kerogens of the Lower-Cambrian Niutitang formation mudstones are dominated by micrinite (more than 95%) which was transferred from amorphous maceral during thermal maturation. Amorphous maceral is a typical maceral in type II kerogen contributed by marine organic matter input (Xiao, 1992). Ro values (>2.5%) suggested that these source rocks were over matured. The maturity parameters, such as Ts/(Ts + Tm), 22S/(22S + 22R) of C_{31}-homohopanes and 20S/(20S + 20R) of C_{29}-regular steranes of the Lower-Cambrian mudstones (YT-1 and SW-8) reached their equilibrium (Table 4). The ratio of C_{23}-tricyclic terpane/C_{30}-$\alpha\beta$ hopane from the Lower-Cambrian mudstone extracts are both lower than 1.0 (Fig. 4). The C_{27}-$\alpha\alpha\alpha$R steranes are the highest in the C_{27}, C_{28} and C_{29}-$\alpha\alpha\alpha$R steranes in both mudstone extracts. It is consistent with the dominant marine organic matter input (Peters et al., 2005a).

The macerals of the Lower-Silurian Longmaxi formation shale are also dominated by micrinite (more than 95%). Micrinite is believed to evolve from amorphous maceral (Xiao, 1992). The TOC value of the Lower-Silurian shale (SW-1) is 1.49%, which is lower than that of the Lower-Cambrian mudstones. Its Ro value is about 2.6%. All of its maturity parameters indicate that it is of high maturity. The C_{23}-tricyclic terpane/C_{30}-$\alpha\beta$ hopane ratio is higher than 1.0 (Fig. 4). The C_{27}-$\alpha\alpha\alpha$R sterane is highest in the C_{27}, C_{28} and C_{29}-$\alpha\alpha\alpha$R steranes.

The thickness of mudstone of the Lower-Permian Qixia formation is very small. The thin mudstone layer of the Lower-Permian Qixia formation (WC-3, $P_1 q$, Type I, 0.76%Ro) contains 2.01% TOC. The organic matter of the Qixia formation is dominated by alginate which indicates marine organic matter input. The Ro value is
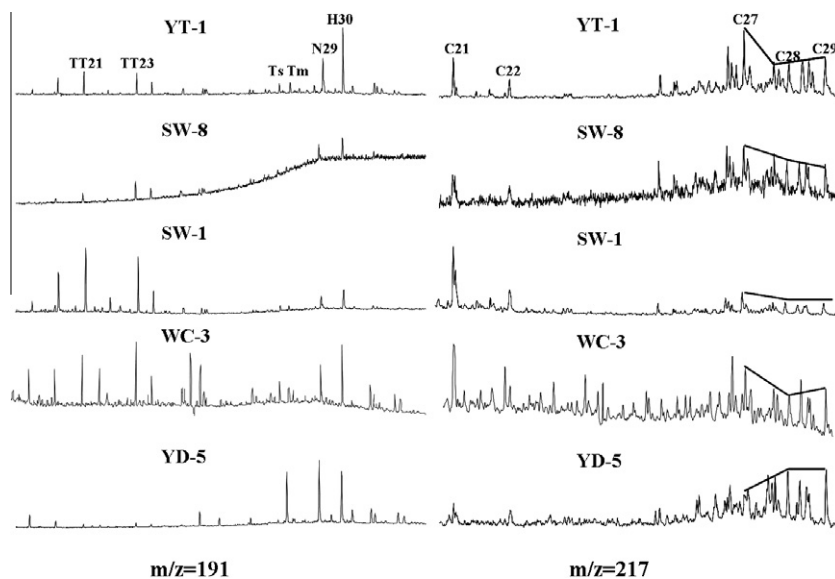
Table 4
The biomarker parameters of the oil seepages, bitumens and source rocks.

Sample	1	2	3	4	5	6	7	8	9	10	11	12
SW-8	3.33	0.45	–	0.58	0.46	0.46	0.27	0.27	–	0.52	0.64	1.97
YT-1	1.40	0.45	0.56	0.55	0.42	0.4	0.28	0.32	0.1	0.53	0.28	2.05
SW-1	0.81	0.51	0.65	0.42	0.39	0.43	0.27	0.3	0.05	0.49	1.94	2.28
WC-3	0.79	–	0.63	0.50	0.37	0.31	0.32	0.37	0.16	0.41	1.63	1.51
YD-5	0.32	0.07	0.59	0.44	0.39	0.16	0.38	0.45	–	1.09	0.08	0.84
KT-1	1.39	0.4	0.61	0.56	0.51	–	–	–	–	1.46	2.13	1.88
KT-2	1.13	0.42	0.55	0.67	0.5	–	–	–	–	1.3	1.33	1.9
KF-2	1.44	–	–	–	–	–	–	–	–	1.04	3.35	1.91
KLMJ-1	4.50	–	–	–	–	–	–	–	–	0.48	1.04	5.21
DY-7	1.70	0.47	0.6	0.48	0.51	0.41	0.29	0.3	–	0.64	1.78	2.38
MJ-1	0.17	0.49	0.56	0.48	0.45	0.44	0.26	0.3	0.08	0.5	0.85	1.22

1: Sat/Aro; 2: Ts/(Ts + Tm); 3: 22S/(22S + 22R) for C_{31}-$\alpha\beta$ homohopanes; 4: 20S/(20S + 20R) for C_{29}-regular steranes; 5: $\beta\beta$/($\beta\beta$ + $\alpha\alpha$) for C_{29}-regular steranes; 6: C_{27}-$\alpha\alpha\alpha$R sterane/(C_{27} + C_{28} + C_{29}-$\alpha\alpha\alpha$R steranes); 7: C_{28}-$\alpha\alpha\alpha$R sterane/(C_{27} + C_{28} + C_{29}-$\alpha\alpha\alpha$R steranes); 8: C_{29}-$\alpha\alpha\alpha$R sterane/(C_{27} + C_{28} + C_{29}-$\alpha\alpha\alpha$R steranes); 9: Gammacerane/C_{30}-$\alpha\beta$ hopane; 10: C_{29}/C_{30}-$\alpha\beta$ hopane; 11: C_{23}-tricyclic terpane/C_{30}-$\alpha\beta$ hopane; 12: pregnane/homopregnane.

Fig. 4. The *m/z* 191 and *m/z* 217 mass chromatograms of the source rocks. Biomarker assignments are listed in Table 3.

0.67%. The C_{23}-tricyclic terpane/C_{30}-$\alpha\beta$ hopane ratio of the Lower-Permian mudstone WC-3 is higher than 1.0 (Fig. 4). C_{29}-$\alpha\alpha\alpha$R sterane is the highest in C_{27}, C_{28} and C_{29}-$\alpha\alpha\alpha$R steranes.

4.2. General geochemical characteristics of the Ordovician–Silurian oil seepages and soft bitumen in the Kaili remnant reservoir

The basic geochemical characteristics and biomarker parameters of the O–S oil seepages KT-1, KT-2 and soft bitumen KF-2 in the Kaili remnant reservoir are shown in Table 1, Table 2 and Table 4. There are broad unresolved complex mixture (UCM) humps in the GC traces of both the saturated hydrocarbon fractions and aromatic hydrocarbon fractions of these samples (Fig. 5). C_{27} and C_{28}-regular steranes are absent in all the three samples (Fig. 6). The relative abundances of pregnane and homopregnane in these samples are higher than C_{27}–C_{29}-regular steranes. Diamondoid hydrocarbons and triaromatic steroid hydrocarbons were detected in all the three samples. All these samples are characterized by the Nor-tricyclic terpanes and Nor-hopanes (Fig. 6). Since tricyclic terpanes are highly resistant to biodegradation (Reed, 1977; Seifert and Moldowan, 1979; Connan et al., 1980), high relative abundance of Nor-tricyclic terpanes and Nor-hopanes and absence of C_{27} and C_{28}-regular steranes usually implies that oil had suffered severe biodegradation. These samples have been biodegraded up

to PM (Peters and Moldowan) level 9 (Peters and Moldowan, 1993a). Thus, the biomarker indexes based on routine biomarkers, such as C_{27}–C_{29}-regular steranes and terpanes, are not valid for the oil-source correlations of the oil seepages and soft bitumen in the Kaili area. Routine maturity biomarker parameters, such as Ts/Tm, isomerization parameters 22S/(22S + 22R) of C_{31}-homohopanes, 20S/(20S + 20R) and $\beta\beta/(\beta\beta + \alpha\alpha)$ of C_{29}-regular steranes, are not valid, either.

Fig. 5 shows the presence of *n*-alkanes in the gas chromatograms of the two severely biodegraded oil seepages (KT-1 and KT-2), this should be the result of mixing of severely biodegraded oil with non-biodegraded oil (Volkman et al., 1983). Diasteranes usually exhibit much higher bioresistance than C_{27}–C_{29}-regular steranes (Seifert and Moldowan, 1979; Requejo and Halpern, 1989). But KT-1 are not dominated by diasteranes even at PM level 9, the C_{29}-regular steranes could be seen in KT-1 and KT-2. This also shows that the two oil seepages were mixtures of severe biodegraded oil and non-biodegraded oil. According to the burial history of Lower-Cambrian Niutitang formation in the eastern Kaili area mentioned below, the Ordovician–Silurian remnant reservoir of the Kaitang village (KT-1 and KT-2) in the Kaili area was likely charged at least twice in the geologic history. The first charged might have suffered severe biodegradation, while the later charged oil has not been biodegraded.
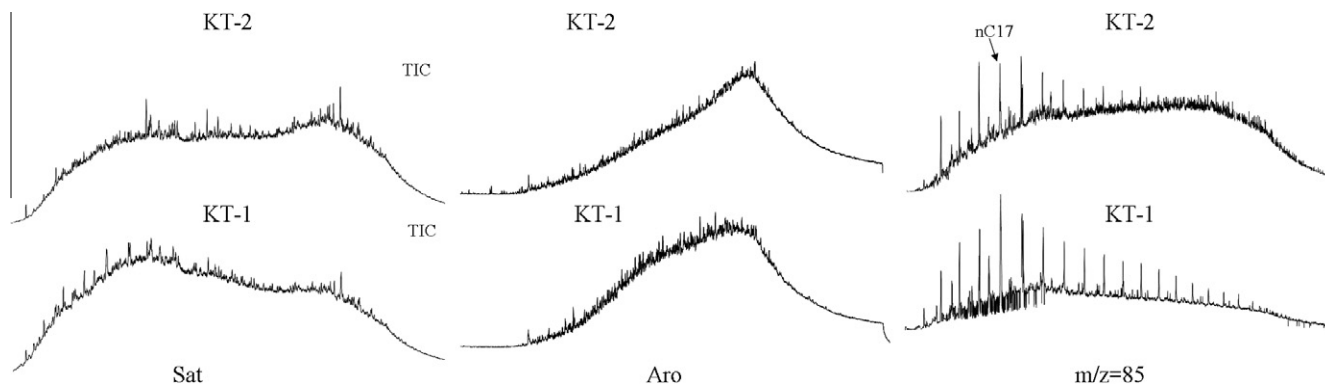

Fig. 5. TIC of saturated and aromatic hydrocarbon and *m/z* 85 mass chromatograms of the O–S oil seepages KT-1 and KT-2.
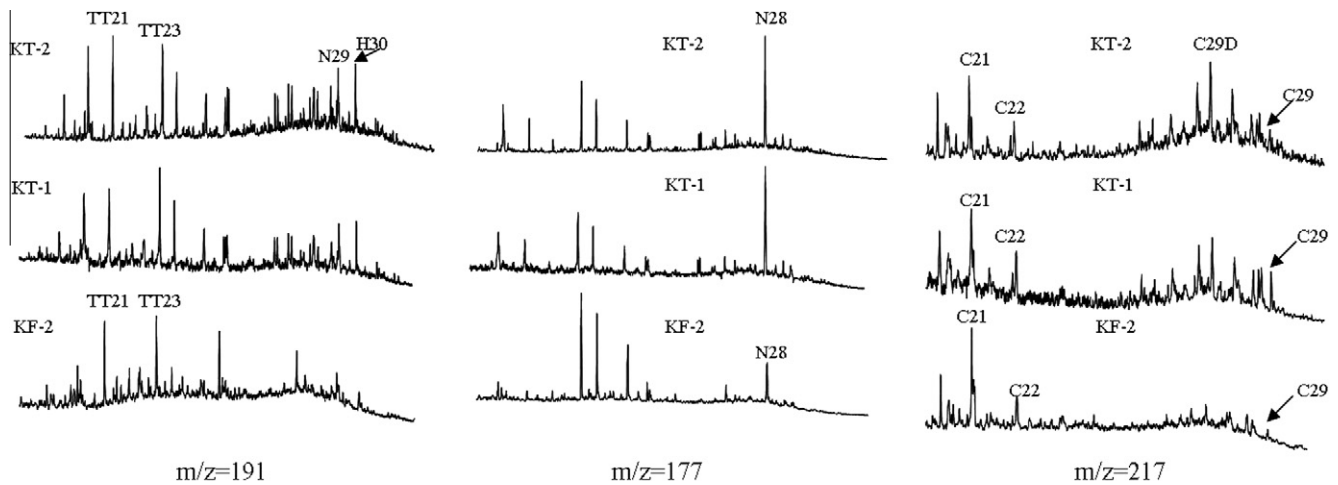
Fig. 6. m/z 191, m/z 177 and m/z 217 Mass chromatograms of the saturated hydrocarbons of the oil seepages and soft bitumen in the Kaili remnant reservoir.

4.3. General geochemical characteristics of the solid bitumens in the Majiang area

The basic geochemical characteristics and biomarker parameters of the solid bitumens in the Majiang area (KLMJ-1 and DY-7 in O₁h) and the Kaili area (MJ-1 in P₁m) are listed in Tables 1, 2 and 4. Slight UCM humps occur in all the three solid bitumen extracts. The n-alkanes of the three solid bitumen extracts were all in the range of C_{13}–C_{28} with the dominance of C_{17} n-alkane (Fig. 7). Due to high maturity, most of the isomerization ratios of the biomarkers in the three solid bitumens have reached equilibrium (Table 4). The C_{23}-tricyclic terpane/C_{30}-$\alpha\beta$ hopane ratio of the extract from DY-7 is up to 1.78 (Fig. 7). Pregnane and homopregnane in DY-7 are higher than C_{27}–C_{29}-regular steranes (Fig. 7, Table 4). The distribution of C_{27}–C_{29}-$\alpha\alpha\alpha R$ steranes in DY-7 bitumen is $C_{27} > C_{29} \geqslant C_{28}$. For the O₁h solid bitumen KLMJ-1, there exist almost no C_{21}–C_{29}-tricyclic terpanes, pentacyclic triterpanes and regular steranes though T_{max} of KLMJ-1 is only 467 °C. For the bitumen in the Lower-Permian reservoir (MJ-1 in P₁m), the C_{23}-tricyclic terpane/C_{30}-$\alpha\beta$ hopane ratio is 0.85. The abundance of C_{27}–C_{29}-regular steranes in MJ-1 is higher than pregnane and homopregnane. The distribution of C_{27}–C_{29}-$\alpha\alpha\alpha R$ steranes in MJ-1 is $C_{27} > C_{29} \geqslant C_{28}$ (Fig. 7).

4.4. Oil–source correlation of the oil seepages and bitumens with possible potential source rocks

Based on the reported data above, there existed extensive biodegradation and thermal cracking in the Majiang paleo-reser-voir and the Kaili remnant reservoir. Therefore, some biomarkers with high resistance to these secondary alterations, such as diamondoid hydrocarbons (Wingert, 1992), triaromatic steroid hydrocarbons (Peters and Moldowan, 1993a; Williams et al., 1986), pregnane and homopregnane (Peters et al., 2005b; Wenger and Isaksen, 2002), were selected for the oil-source correlations. Since diamondoid hydrocarbons are highly resistant to severe thermal alteration and biodegradation after oil expulsion (Wingert, 1992; Grice et al., 2000), they are useful for oil-oil correlation in cases where the oil and bitumen have suffered severe biodegradation or thermal cracking (Schulz et al., 2001). Pregnane and homopregnane are also highly resistant to biodegradation. However, they can be altered by severe thermal degradation (Huang et al., 1994). Thus, pregnane and homopregnane could be useful indicators for the oil-oil correlation of the oil seepages and soft bitumen with low maturity in the Kaili area. Triaromatic steroids are highly resistant to biodegradation even at PM level 9 (Peters and Moldowan, 1993a). Thus they are also useful indicators for the oil-oil and oil-source correlation in the Kaili area.

The stable carbon isotopic composition of individual n-alkanes is a useful tool in oil-oil and oil-source correlation (Bjorøy et al., 1991). Neither biodegradation nor thermal maturation can change $\delta^{13}C$ values of n-alkanes or whole oil very much (Mansuy et al., 1997; Mazeas et al., 2002). The stable carbon isotopic distribution of individual n-alkanes in the asphaltene pyrolysates can be used as a correlation tool for severely biodegraded oils (Xiong and Geng, 2000). All these indexes above are comprehensively used here for oil–oil correlation and oil–source correlations.
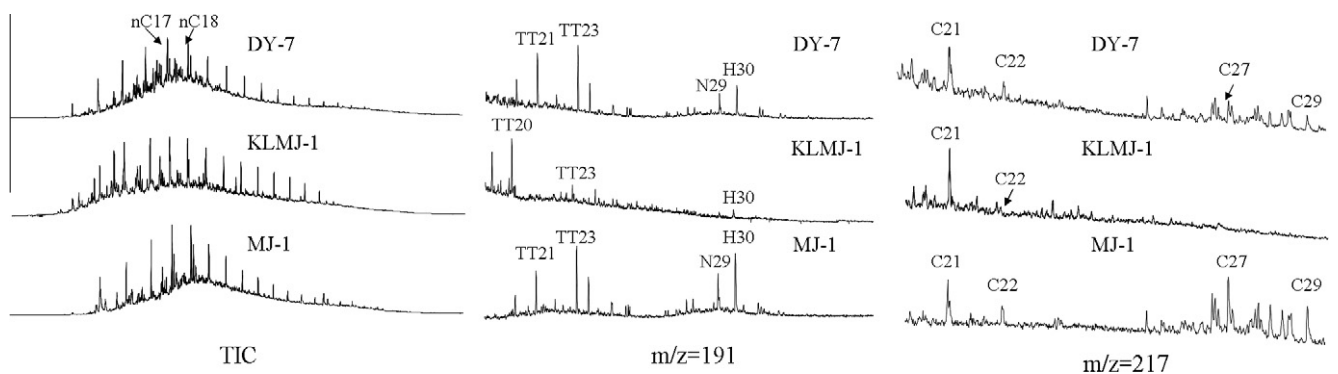

Fig. 7. TIC, m/z 191 and m/z 217 mass chromatograms of the solid bitumens in the Majiang paleo-reservoir.

4.4.1. Terpanes and regular steranes

Due to severe biodegradation and thermal alteration, oil–oil and oil–source correlations only based on routine biomarkers such as terpanes and C_{27}–C_{29}-regular steranes may be misleading. For example, tricyclic terpanes are more resistant to biodegradation than hopanes (Reed, 1977; Seifert and Moldowan, 1979; Connan et al., 1980), so the ratio of C_{23}-tricyclic terpane/C_{30}-αβ hopane in non-biodegraded oils or slightly biodegraded oils would be lower than that of severely biodegraded oils. The hopanes of the Ordovician–Silurian oil seepages and soft bitumen in the Kaili area were significantly altered so that the C_{23}-tricyclic terpane/C_{30}-αβ hopane ratio should be altered during biodegradation. As a consequence, although the ratio of C_{23}-tricyclic terpane/C_{30}-αβ hopane in the oil seepages (KT-1 and KT-2) and soft bitumen (KF-2) are more similar to that in the Lower-Permian source rocks than that in the Lower-Cambrian source rocks, conclusion cannot be made that the oil seepages and soft bitumen came from the Lower-Permian source rocks. Traditionally, the distribution of C_{27}, C_{28} and C_{29}-αααR steranes is used to differentiate crude oils from various source rocks or from different organic input in the same source rocks (Moldowan et al., 1985; Peters and Moldowan, 1993b; Czochanska et al., 1988). However, the C_{27}–C_{28}-regular steranes are absent in the Ordovician–Silurian oil seepages KT-1 and KT-2 and soft bitumen KF-2 in the Kaili area because of the severe biodegradation. C_{27}–C_{29}-regular steranes are also absent in the solid bitumen KLMJ-1. Furthermore, the distributions of C_{27}, C_{28} and C_{29}-αααR steranes in the Lower-Cambrian mudstones, Lower-Silurian shale, Lower-Permian mudstones, Lower-Permian solid bitumen MJ-1 and Lower-Ordovician bitumen DY-7 are quite similar, all indicating a distribution of $C_{27} > C_{29} \geqslant C_{28}$. Thus, the distributions of C_{27}–C_{29}-αααR steranes cannot provide enough information for the oil-source correlations in the study area.

It is commonly known that pregnanes are derived from the hormones, pregnanol and pregnanone (Huang et al., 1984; De Leeuw and Bass, 1986). Pregnane and homopregnane may also be produced by thermal cracking of C_{27}–C_{29}-regular steranes (Huang et al., 1994). The contents of pregnane and homopregnane may be influenced by thermal cracking. However, pregnane and homopregnane are both highly resistant to biodegradation (Wenger and Isaksen, 2002). Thus, the pregnane/homopregnane ratios of severe biodegraded oils with the same low maturity from the same source rock should be close to each other. The ratio might be an assistant for the oil-source correlation in this case. The oil seepages KT-1, KT-2 and soft bitumen KF-2 have similar thermal maturity (Ro < 1%). If the pregnane/homopregnane ratios are very close to each other, they would be from the same source. Actually, the pregnane/homopregnane ratios of the two Ordovician–Silurian oil seepages (KT-1 and KT-2) are both about 1.9, which is very close to the Lower-Ordovician soft bitumen KF-2 (Table 4). Thus, the Ordovician–Silurian oil seepages and soft bitumen in the Kaili area are likely generated by the same source rock.

4.4.2. Dimethyl diamantanes

The distributions of 4,9-DMD, 4,8-DMD and 3,4-DMD in samples KT-1, KT-2, KF-2, KLMJ-1 and DY-7 from the Ordovician–Silurian reservoirs, are quite similar and different from that in solid bitumen MJ-1 from the Lower-Permian reservoir (Fig. 8). The abundances of 4,8-DMD are obviously lower than that of 3,4-DMD in all the Ordovician–Silurian oil seepages and bitumens, while the abundance of 4,8-DMD is close to that of 3,4-DMD in the Lower-Permian solid bitumen MJ-1 (Fig. 9). Thus, the Ordovician–Silurian oil seepages and Lower-Ordovician bitumens in both the Kaili area and the Majiang area are likely generated by the same source rock. The Lower-Permian solid bitumen MJ-1 should have a different source rock.
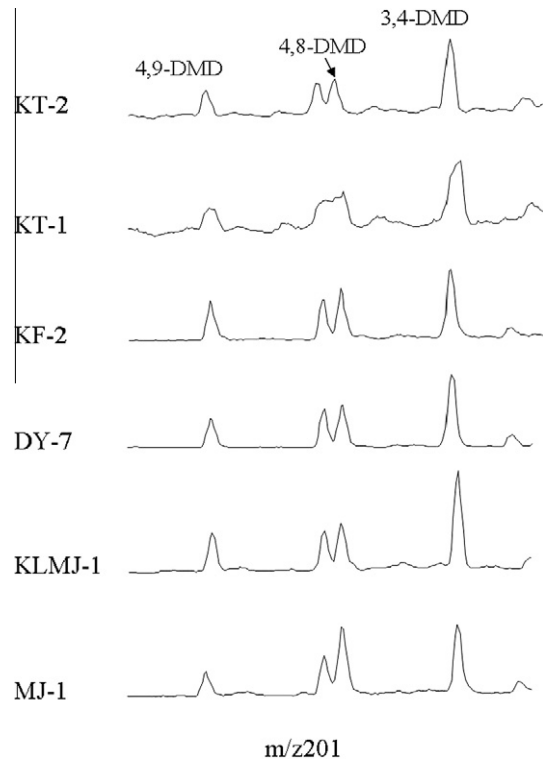

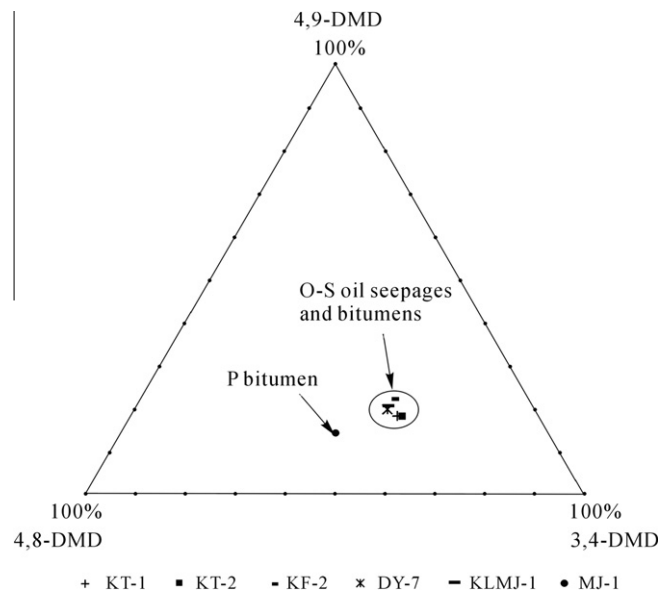**Fig. 8.** *m/z* 201 mass chromatograms of the oil seepages and bitumens.

Fig. 9. Triangular plot of the distribution of 4,9-DMD, 4,8-DMD and 3,4-DMD in the oil seepages and bitumens.

4.4.3. Bulk $\delta^{13}C$ values

The bulk $\delta^{13}C$ values of kerogens from the Lower-Cambrian mudstones in the study area ranged from −29.1‰ to −34.7‰ (most of them in −31.1‰ to −34.7‰), while those of Permian source rocks ranged from −22.7‰ to −29.2‰ (most of them in −22.7‰ to −27.7‰) (Fig. 10, Table 1). The bulk $\delta^{13}C$ values of the Ordovician–Silurian oil seepages (KT-1 and KT-2) and Lower-Ordovician bitumens (KF-2, KLMJ-1, DY-7) are all in the narrow range of −32.2‰ to −32.3‰, which is the range of values obtained in kerogens from the Lower-Cambrian mudstones (Fig. 10, Table 1).
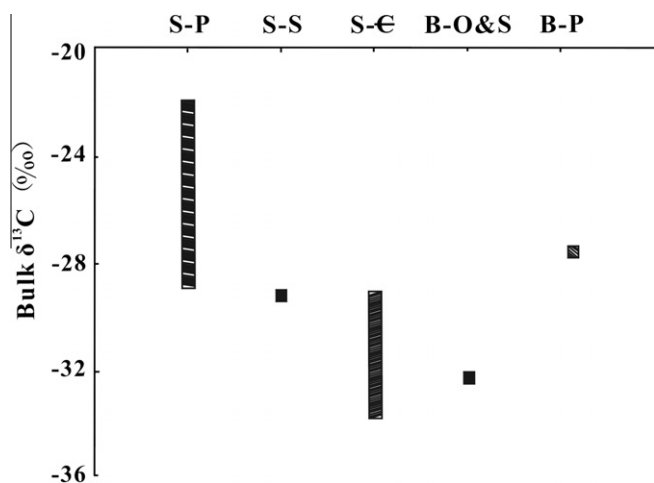
Fig. 10. The bulk $\delta^{13}C$ values of the kerogens, bitumens and oil seepages*. S–P: the Lower-Permian source rock kerogens; S–S: the Lower-Silurian source rock kerogens; S–∈: the Lower-Cambrian source rock kerogens; B–O&S: the Ordovician–Silurian oil seepages and Lower-Ordovician bitumens; B–P: the bitumen in Lower-Permian reservoir. * Some of the bulk $\delta^{13}C$ values of the source rock kerogens are from Wuxi Institute of Petroleum Geology of SINOPEC.

The bulk $\delta^{13}C$ values of the Lower-Permian solid bitumen (MJ-1, −27.9‰) are in the range obtained in kerogens from the Permian source rocks. The kerogens of Permian source rocks are much heavier (rich in $\delta^{13}C$) than the oil seepages and bitumens from the Ordovician–Silurian reservoir.

4.4.4. $\delta^{13}C$ values of individual n-alkanes

n-Alkanes were still detected in the Ordovician–Silurian oil seepages KT-1 and KT-2 (Figs. 5 and 6). As mentioned above, it should be due to mixing of severely biodegraded oil and non-biodegraded oil. The $\delta^{13}C$ values of the individual n-alkanes from the oil seepages and their asphaltene pyrolysates were compared to see whether the severely biodegraded oil came from the same source rock as the non-biodegraded oil. The $\delta^{13}C$ values of the individual n-alkanes from oil seepages, bitumens, source rock extracts and asphaltene pyrolysates are plotted in Fig. 11. The $\delta^{13}C$ values are in the range of −33.0‰ to −33.8‰ for the free n-alkanes in
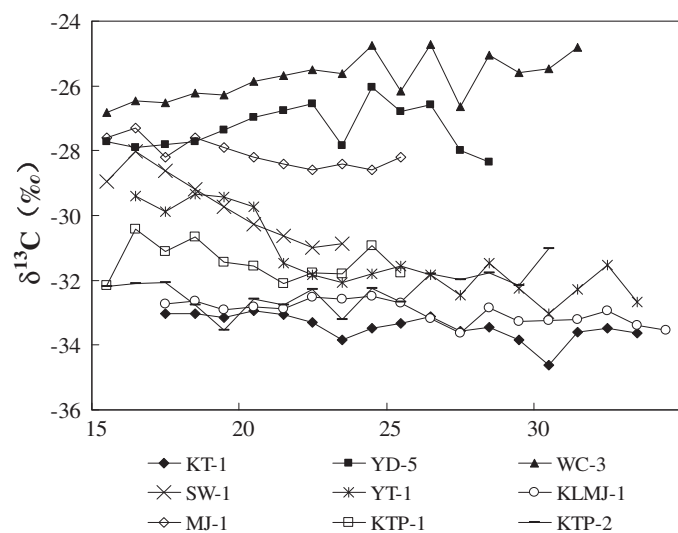

Fig. 11. The $\delta^{13}C$ values of individual n-alkanes in bitumens, asphaltene pyrolysates and source rock extracts. KTP-1: asphaltene pyrolysates of KT-1; KTP-2: asphaltene pyrolysates of KT-2.

oil seepage KT-1, and in the range of −30.4‰ to −33.5‰ for the n-alkanes in the asphaltene pyrolysates of oil seepages KT-1 and KT-2. Thus, both the non-biodegraded oil and severely biodegraded oil in the Ordovician–Silurian reservoir of the Kaili area were sourced from the same source rock.

The $\delta^{13}C$ values of the individual n-alkanes from the extracts of the Lower-Silurian shale (SW-1), Lower-Permian mudstone (WC-3) and coal (YD-5) are in the range of −28.0‰ to −31.0‰, −24.8‰ to −26.8‰ and −26.5‰ to −28.3‰, respectively. Contrarily, the $\delta^{13}C$ values of the individual n-alkanes from the Lower-Cambrian mudstones are all in the range of −29.4‰ to −32.7‰, much closer to that of the Ordovician–Silurian oil seepages (KT-1 and KT-2) and Lower-Ordovician bitumens (KF-2, DY-7, KLMJ-1) than that of the Lower-Permian source rocks (Fig. 11). The stable carbon isotopic compositions of the individual n-alkanes (C_{21}–C_{33}) in the Ordovician–Silurian oil seepages are lighter, in the range of 1.0–2.0‰, than that of Lower-Cambrian mudstones. n-alkanes become isotopically heavier with increasing thermal maturity (Bjorøy et al., 1991; Galimov, 2006). As the thermal maturity of the Lower-Cambrian mudstones are higher than that of the Ordovician–Silurian oil seepages, the difference between them could be attributed to the difference in thermal maturity. In addition, the $\delta^{13}C$ values of the n-alkanes in the Lower-Permian bitumen MJ-1 are in the range of −26.1‰ to −28.6‰, which are quite close to those of the Lower-Permian mudstone.

4.4.5. Triaromatic steroid hydrocarbons

It is commonly accepted that triaromatic steroid hydrocarbons are the products of steranes aromatization and derived from marine Acritarchs whose precursor was Dinophyceae (Liang and Chen, 2005; Zhang et al., 2002; Peters et al., 2005c). Triaromatic steroid hydrocarbons are the kind of biomarkers with highest bioresistance to severe biodegradation (Peters and Moldowan, 1993a). The distributions of the triaromatic steroid hydrocarbons in the Ordovician–Silurian oil seepages (KT-1 and KT-2) and soft bitumen KF-2 are quite similar (Figs. 12 and 13). The concentrations of C_{20} (1TA20) and C_{21}-triaromatic steroids (1TA21) are lower than that of C_{26}–C_{28}-triaromatic steroids. C_{28}-triaromatic steroid (5TA28 + 7TA28) is dominant in the triaromatic steroids of all the three samples. For those Lower-Cambrian marine mudstone samples, C_{20}-triaromatic steroid is the dominant triaromatic steroid. C_{20}–C_{21}-triaromatic steroids are more vulnerable in biodegradation compared to C_{26}–C_{28}-triaromatic steroids (Wardroper et al., 1984). Meanwhile, the increase of thermal maturity could also lead to the decrease in the values of C_{26}–C_{28}-triaromatic steroids/C_{20}–C_{21}-triaromatic steroids within the oils and bitumens (Mackenzie et al., 1982; Riolo et al., 1985). Thus, the differences in concentrations of C_{20} (1TA20) and C_{21} (1TA21) triaromatic steroid between the Ordovician–Silurian samples (KT-1, KT-2 and KF-2) and Lower-Cambrian mudstone (YT-1) can be attributed to the difference in their maturity and biodegradation degree. Triaromatic steroids were not detected in the Lower-Silurian (S_1l) shale SW-1 and Lower-Permian (P_1q) mudstone WC-3. The Ordovician–Silurian oil seepages and soft bitumen are likely to be mainly sourced from the Lower-Cambrian mudstones rather than from the Lower-Permian mudstone and the Lower-Silurian shale.

Based on the distributions of dimethyl diamantanes and triaromatic steroid hydrocarbons, the pregnane/homopregnane values, the bulk $\delta^{13}C$ values of kerogens and bitumens and the $\delta^{13}C$ values of individual n-alkanes, the Lower-Cambrian mudstones ($\in_1 n$) were likely to be the main source rocks of the oil seepages and bitumens from the Ordovician–Silurian reservoirs in both the Majiang area and the Kaili area, while the solid bitumen in the Lower-Permian reservoir (MJ-1 in P_1m) should be sourced from the Lower-Permian mudstone (P_1q).
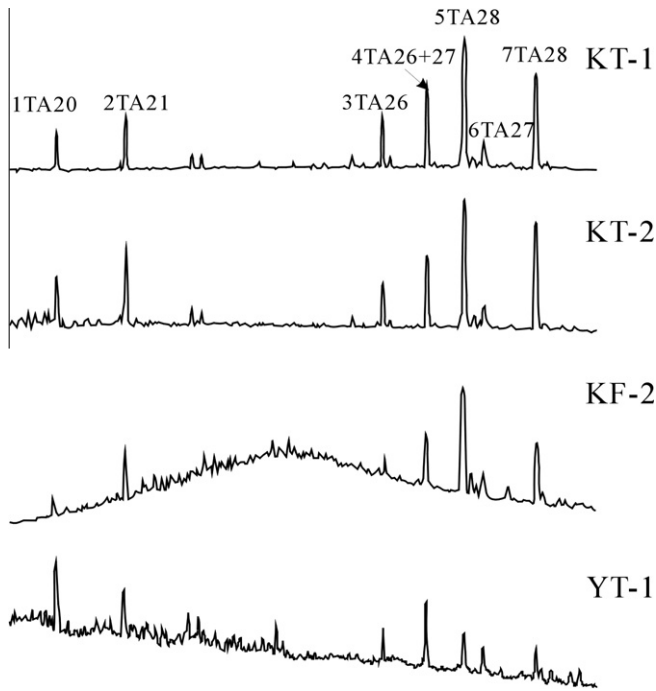
Fig. 12. m/z 231 mass chromatograms displaying triaromatic steroids of the oil seepages, bitumen and $\in_1 n$ mudstone extract.
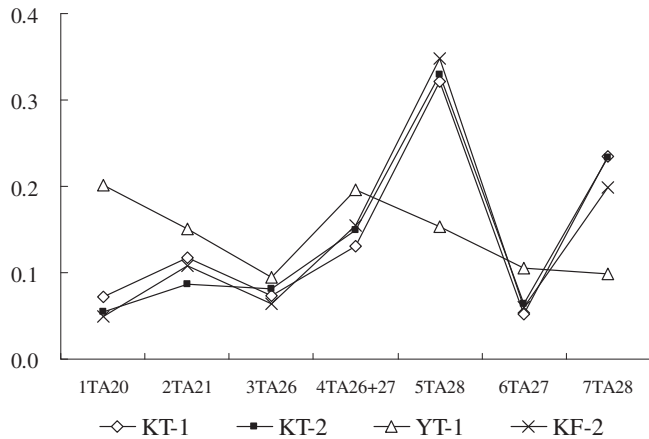

Fig. 13. The distributions of triaromatic steroids in the extract of $\in_1 n$ mudstone, O–S oilseepages and bitumen. 1TA20: C_{20}-triaromatic steroid; 2TA21: C_{21}-triaromatic steroid; 3TA26: C_{26}-S-triaromatic steroid; 4TA26 + 27: C_{26}R-triaromatic steroid + C_{27}-S-triaromatic steroid; 5TA28: C_{28}-S-triaromatic steroid; 6TA27: C_{27}-R-triaromatic steroid; 7TA28: C_{28}-R-triaromatic steroid.
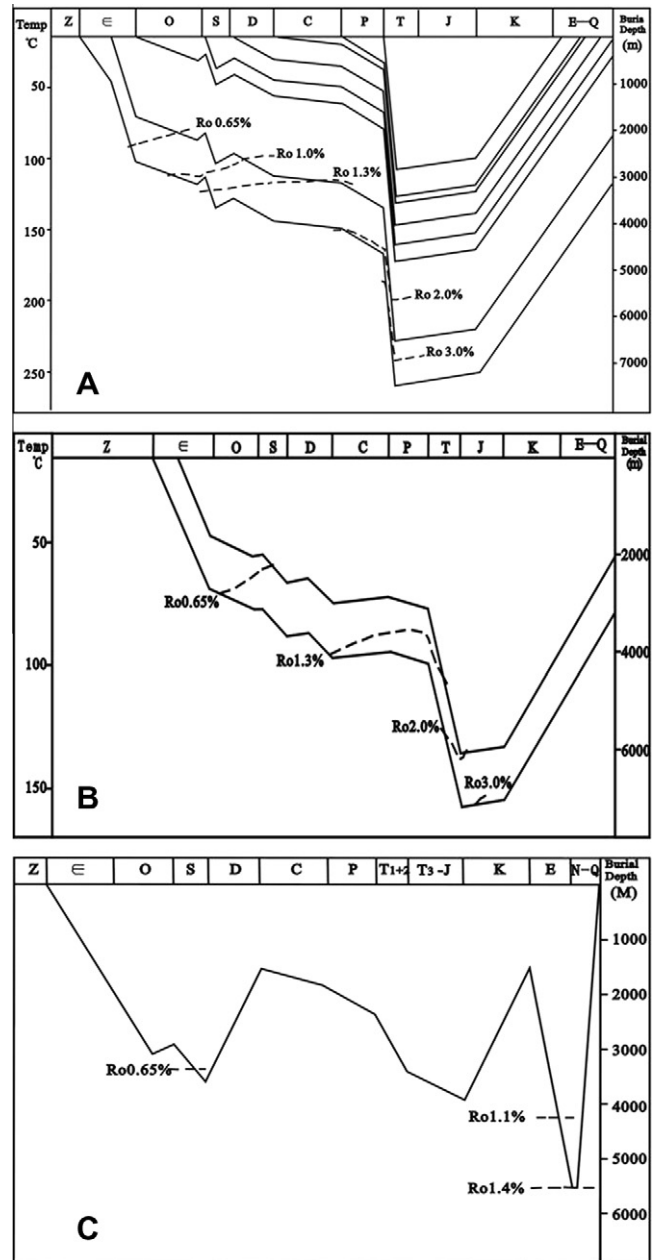

Fig. 14. The evolution thermal maturity of the Lower-Cambrian source rocks in: (A) the Majiang area (Li et al., 2003); (B) the western Kaili area (Ma et al., 2004); and (C) the eastern Kaili area (Ma et al., 2004).

4.5. Oil charge history and reservoir evolution of the Majiang paleo-reservoir and the Kaili remnant reservoir

The maturity of the source rocks in the Majiang area, the western Kaili area and the eastern Kaili area are quite different in the Southern Guizhou Depression. In the Majiang area, the Lower-Cambrian mudstones entered oil window between Late Cambrian and Early Ordovician (Fig. 14A), and reached their oil generation peak between Late Ordovician and Early Devonian (Li et al., 2003). The maximum burial depth of the Lower-Cambrian mudstones exceeded 7000 meters, and the Ro values of the Lower-Cambrian mudstones exceeded 3.0% (Ma et al., 2004). Due to strong uplift and erosion during Yanshanian orogeny and Himalayan orogeny, the Lower-Cambrian Niutitang formation was out-cropped. The Ordovician–Silurian reservoirs in the Majiang area were also outcropped and destroyed and finally occurred as paleo-reservoirs today.

The tectonic evolution in the western Kaili area was quite similar to that in the Majiang area. The maximum burial depth of the Lower-Cambrian mudstones in the western Kaili area is about 7000 m, and the vitrinite reflectance values of the source rocks exceeds 2.5% (Fig. 14B) (Ma et al., 2004). In the eastern Kaili area such as the Taijiang area, the Lower-Cambrian mudstones have much lower maturities. In fact, the maturities of the Lower-Cambrian and Lower-Permian source rocks decrease gradually from west to east in the whole Southern Guizhou Depression due to the decrease in the maximum burial depth in the geologic history. The Lower-Cambrian mudstones in the eastern Kaili area have been subsided and uplifted for three times. The source rocks were first

subsided and entered oil window at Silurian, and then were quickly uplifted (Fig. 14C). In Indosinian orogeny, the source rocks entered oil window again and were uplifted at Cretaceous. In Himalayan orogeny, the Lower-Cambrian mudstones were deeply buried for a third time, and the ultimate Ro values of the source rocks reached about 1.4%. Finally, the Lower Paleozoic strata of the eastern Kaili area were uplift at Miocene, both the Lower-Cambrian mudstones and the Ordovician–Silurian reservoirs were outcropped. The burial history of the Lower-Cambrian mudstones in the eastern Kaili area and the geochemical characteristics of the Ordovician–Silurian oil seepages in the Kaili area indicated that Ordovician–Silurian reservoir of the Kaili area, especially in the eastern part, was likely charged at least twice by the oil from the Lower-Cambrian mudstones. The Lower-Cambrian mudstones of the western Kaili area reached oil generation peak at Early Devonian, while the same mudstones of the eastern Kaili area had not reached oil generation peak until Late Eocene. Thus, the Ordovician–Silurian reservoir (KT-1 and KT-2) of Kaitang village in the Eastern Kaili area was first charged by oil generated from the Lower-Cambrian mudstones of the western Kaili area since Early Devonian. Due to low reservoir temperature, the Kaili Ordovician–Silurian reservoir was not pasteurized and biodegradation was likely to occur (Wilhelms et al., 2001). The oil reservoir was then pasteurized at higher temperature due to continued increase of the burial depth. The Ordovician–Silurian reservoir was charged again by the oil generated from the Lower-Cambrian mudstones in the eastern Kaili area between Eocene and Pliocene. The oil charged later was not biodegraded. Thus the crude oil of the Kaili remnant reservoir is characterized by the mixing of biodegraded oil and non-biodegraded oil.

5. Conclusion

(1) The oil seepages from the O–S reservoir of Kaitang village, belonging to the Kaili remnant reservoirs, were mixing oils of severely biodegraded oil and non-biodegraded oil. Both the biodegraded oil and non-biodegraded oil in the O–S reservoir of the the Kaili area were mainly sourced from the Lower-Cambrian mudstones ($\in_1 n$). The O–S reservoir in the Kaili area might have been charged at least twice, first by the oil from the source rocks of the western Kaili area and then by the oil from the source rocks of the eastern part. The first charged oil was biodegraded while the later was not biodegraded.

(2) Evidence from the biomarker parameters resistant to secondary alterations, the bulk δ^{13}C values of kerogens of source rocks, oil seepages and bitumens, and the δ^{13}C values of individual n-alkanes reveal that the oil seepages and bitumens in the Kaili O–S remnant reservoirs and the Lower-Ordovician solid bitumens in the Majiang paleo-reservoirs were all mainly sourced from the Lower-Cambrian mudstones, but the contribution of other source rocks can not be totally excluded.

Acknowledgements

References

Bjorøy, M., Hall, K., Gillyon, P., Jumeau, J., 1991. Carbon isotope variations in n-alkanes and isoprenoids of whole oils. Chemical Geology 93, 13–20.

Chen, Y., Zhang, H., Li, X., Chu, L., Zhang, W., Deng, W., Huang, C., 2006. Sedimentary and structural evolution and oil-gas exploration direction in Jiangnan-Xuefeng structural belt and its edge. South China Oil & Gas 72, 5–10 (in Chinese with English abstract).

Connan, J., Restle, A., Albrecht, P., 1980. Biodegradation of crude oil in the Aquitaine basin. Physics and Chemistry of the Earth 12, 1–17.

Czochanska, Z., Gilbert, T.D., Philp, R.P., Sheppard, C., Weston, R.J., Wood, T.A., Woolhouse, A.D., 1988. Geochemical application of sterane and triterpane biomarkers to a description of oils from the Taranaki Basin in New Zealand. Organic Geochemistry 12, 123–135.

De Leeuw, J.W., Bass, M., 1986. Early diagenesis of steroids. In: Johns, R.B. (Ed.), Biological Markers in the Sedimentary Record. Elsevier, Amsterdam, pp. 102–127.

Ding, D., Liu, G., Chen, Y., Pan, W., Qu, C., Rao, D., 2007. Hydrocarbon accumulation and oil–source correlation in the front of Jiangnan-Xuefeng mountain: series 3 of the southern structure studies. Petroleum Geology & Experiment 29, 345–354 (in Chinese with English abstract).

Galimov, E.M., 2006. Isotope organic geochemistry. Organic Geochemistry 37, 1200–1262.

Grice, K., Alexander, R., Kagi, R.I., 2000. Diamondoid hydrocarbon ratios as indicators of biodegradation in Australian crude oils. Organic Geochemistry 31, 67–73.

Hu, Y., Han, R., Mao, X., 2007. Relationship between metal mineral ization and accumulation of oil and gas in the eastern Guizhou. Geology and Prospecting 43 (5), 51–56 (in Chinese with English abstract).

Huang, D., Li, J., Zhou, Z., Gu, X., Zhang, D., 1984. Evolution and Hydrocarbon-Generating Mechanism and Non-marine Organic Matter. Petroleum Industry Press, Beijing.

Huang, D., Zhang, D., Li, J., 1994. The origin of 4-methyl steranes and pregnanes from tertiary strata in the Qaidam Basin, China. Organic Geochemistry 22, 343–348.

Jacob, H., 1985. Disperse solid bitumens as an indicator for migration and maturity in prospecting for oil and gas. Erdöl und Kohle-Erdgas 38, 365.

Li, C., Wu, Z., Zhang, Z., Chen, G., 2003. The Study of Paleo-reservoir and Remnant Reservoir in the Southern Guizhou Depression of China, pp. 35–38 (Report from Sinopec Exploration Southern Company, in Chinese).

Li, Z., Luo, Z., Liu, S., Yong, Z., 2006. Assessment of petroleum resources in Lower Assemblage (Z–S) under Xuefeng thrust nappe. Oil & Gas Geology 27 (3), 392–398 (in Chinese with English abstract).

Liang, D., Chen, J., 2005. Oil–source correlations for high and over matured marine source rocks in South China. Petroleum Exploration and Development 32 (2), 8–14 (in Chinese with English abstract).

Liao, Y., Geng, A., Xiong, Y., Liu, D., Lu, J., Liu, J., Zhang, H., Geng, X., 2004. The influence of hydrocarbon expulsion on carbon isotopic compositions of individual n-alkanes in pyrolysates of selected terrestrial kerogens. Organic Geochemistry 35, 1479–1488.

Liao, Y., Geng, A., Huang, H., 2009. The influence of biodegradation on resins and asphaltenes in the Liaohe Basin. Organic Geochemistry 40, 312–320.

Liu, Y., Shen, Z., Ding, D., Leng, D., Liu, G., Rao, D., 2008. The characters of the old asphalt–oil pool in the Jiangnan-Xuefeng thrust nappe front and the correlation of oil sources. Journal of Chengdu University of Technology (Science & Technology Edition) 35 (1), 34–40 (in Chinese with English abstract).

Ma, L., Chen, H., Gan, K., Xu, K., Xu, X., Wu, G., Ye, Z., Liang, X., Wu, S., Qu, Y., Zhang, P., Ge, P., 2004. Geotectonics and petroleum geology of marine sedimentary rocks in southern China. Geological Publishing House, Beijing, China. pp. 513–534.

Mackenzie, A.S., Lamb, N.A., Maxwell, J.R., 1982. Steroid hydrocarbons and the thermal history of sediments. Nature 295, 223–226.

Mansuy, L., Philp, R.P., Allen, J., 1997. Source identification of oil spills based on the isotopic composition of individual components in weathered oil samples. Environmental Science and Technology 31, 3417–3425.

Mazeas, L., Budzinski, H., Raymond, N., 2002. Absence of stable carbon isotope fractionation of saturated and polycyclic aromatic hydrocarbons during aerobic bacterial biodegradation. Organic Geochemistry 33, 1259–1272.

Moldowan, J.M., Seifert, W.K., Gallegos, E.J., 1985. Relationship between petroleum composition and depositional environment of petroleum source rock. AAPG Bulletin 69, 1255–1268.

Peters, K.E., Moldowan, J.M., 1993a. The Biomarker Guide: Interpreting Molecular Fossils in Petroleum and Ancient Sediments. Prentice Hall, New Jersey. pp. 253–254.

Peters, K.E., Moldowan, J.M., 1993b. The Biomarker Guide: Interpreting Molecular Fossils in Petroleum and Ancient Sediments. Prentice Hall, New Jersey. pp. 182–186.

Peters, K.E., Walters, C.C., Moldowan, J.M., 2005a. The Biomarker Guide II: Biomarkers and Isotopes in Petroleum Systems and Earth History, second ed. Cambridge University Press, Cambridge. pp. 499–586.

Peters, K.E., Walters, C.C., Moldowan, J.M., 2005b. The Biomarker Guide II Biomarkers and Isotopes in Petroleum Systems and Earth History, second ed. Cambridge University Press, Cambridge. pp. 674–675.

Peters, K.E., Walters, C.C., Moldowan, J.M., 2005c. The Biomarker Guide II: Biomarkers and Isotopes in Petroleum Systems and Earth History, second ed. Cambridge University Press, Cambridge. pp. 698–699.

Reed, W.E., 1977. Molecular compositions of weathered petroleum and comparison with its possible source. Geochimica et Cosmochimica Acta 41, 237–247.

Requejo, A.G., Halpern, H.I., 1989. An unusual hopane biodegradation sequence in tar sands from the Point Arena (Monterey) Formation. Nature 342, 670–673.

Riolo, J., Hussler, G., Albrecht, P., Connan, J., 1985. Distribution of aromatic steroids in geological samples: their evaluation as geochemical parameters. Organic Geochemistry 10, 981–990.

Schulz, L.K., Wilhelms, A., Rein, E., Steen, A.S., 2001. Application of diamondoids to distinguish source rock facies. Organic Geochemistry 32, 365–375.

Seifert, W.K., Moldowan, J.M., 1979. The effect of biodegradation on steranes and terpanes in crude oils. Geochimica et Cosmochimica Acta 42, 77–95.

Tenger, Qin, J., Zheng, L., 2008. Hydrocarbon potential on excellent hydrocarbon source rock in Southern Guizhou depression and its spacial-temporal distribution. Acta Geologica Sinica 82, 366–372 (in Chinese with English abstract).

Tian, H., Guo, T., Hu, D., Tang, L., Wo, Y., Song, L., Yang, Z., 2006. Marine Lower Assemblage and exploration prospect of Central Guizhou Uplift and its adjacent areas. Journal of Palaeogeography 8 (4), 509–518 (in Chinese with English abstract).

Volkman, J.K., Alexander, R., Kagi, R.I., Noble, R.A., Woodhouse, G.W., 1983. A geochemical reconstruction of oil generation in the Barrow Sub-basin of Western Australia. Geochimica et Cosmochimica Acta 47, 2091–2106.

Wardroper, A.M.K., Hoffmann, C.F., Maxwell, J.R., Barwise, A.J.G., Goodwin, N.S., Park, P.J.D., 1984. Crude oil biodegradation under simulated and natural conditions—II. Aromatic steroid hydrocarbons. Organic Geochemistry 6, 605–617.

Wenger, L.M., Isaksen, G.H., 2002. Control of hydrocarbon seepage intensity on level of biodegradation in sea bottom sediments. Organic Geochemistry 33, 1277–1292.

Williams, J.A., Bjorøy, M., Dolcater, D.L., Winters, J.C., 1986. Biodegradation in South Texas Eocence oil: effects on aromatics and biomarkers. Organic Geochemistry 10, 451–462.

Wilhelms, A., Larter, S.R., Head, I., Farrimond, P., di-Primio, R., Zwach, C., 2001. Biodegradation of oil in uplifted basins prevented by deep-burial sterilization. Nature 411, 1034–1037.

Wingert, W.S., 1992. GC–MS analysis of diamondoid hydrocarbons in smackover petroleum. Fuel 71, 37–43.

Wu, W., 1989. The formation and destruction of palaeo-oil-reservoirs in the east of Guizhou province. Geology of Guizhou 18, 9–22 (in Chinese with English abstract).

Xiao, X., 1992. Application of organic petrology in petroleum and gas source rock evaluation. Guangdong Science and Technology Press, Guangzhou, China (pp. 68–69, in Chinese).

Xiong, Y., Geng, A., 2000. Carbon isotopic composition of individual n-alkanes in asphaltene pyrolysates of biodegraded crude oils from the Liaohe Basin, China. Organic Geochemistry 31, 1441–1449.

Zhai, G., Wang, S., Shi, X., Qiu, Z., Zha, Q., Hu, J., 1987. Petroleum Geology of China, vol. 11. Petroleum Industry Press, Beijing, China (pp. 172–189, in Chinese).

Zhang, S., Bian, L., He, Z., Wang, D., Zhang, B., Moldowan, J.M., Li, M., Wang, F., 2002. The abnormal distribution of the molecular fossils in the pre-Cambrian and Cambrian: its biological significance. Science in China (Series D) 45, 3–10.

Zhang, Q., Tenger, Zhang, Z., Qin, J., 2007. Oil source of oil seepage and solid bitumen in the Kaili–Majiang Area. Acta Geologica Sinica 81 (8), 1118–1124 (in Chinese with English abstract).